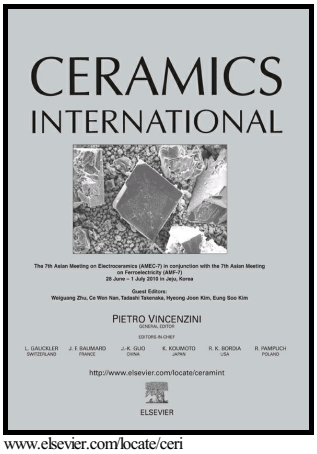

www.elsevier.com/locate/ceri

New strategy for microplastic degradation: green photocatalysis using a protein-based porous N-TiO_2 semiconductor

Maria Camila Ariza-Tarazona, Juan Francisco Villarreal-Chiu, Virginia Barbieri, Cristina Siligardi, Erika Iveth Cedillo-González

PII: S0272-8842(18)33009-8
DOI: https://doi.org/10.1016/j.ceramint.2018.10.208
Reference: CERI19920

To appear in: *Ceramics International*

Received date: 28 July 2018
Revised date: 10 October 2018
Accepted date: 24 October 2018

Cite this article as: Maria Camila Ariza-Tarazona, Juan Francisco Villarreal-Chiu, Virginia Barbieri, Cristina Siligardi and Erika Iveth Cedillo-González, New strategy for microplastic degradation: green photocatalysis using a protein-based porous N-TiO_2 semiconductor, *Ceramics International,* https://doi.org/10.1016/j.ceramint.2018.10.208

New strategy for microplastic degradation: green photocatalysis using a protein-based porous N-TiO_2 semiconductor

Maria Camila Ariza-Tarazona[a,*], Juan Francisco Villarreal-Chiu[b], Virginia Barbieri[c], Cristina Siligardi[c], Erika Iveth Cedillo-González[a]

[a]Universidad Autónoma de Nuevo León, Facultad de Ciencias Químicas, Departamento de Ingeniería Química. Av. Universidad S/N Ciudad Universitaria, San Nicolás de los Garza, Nuevo León. 66455. México.

[b]Universidad Autónoma de Nuevo León, Facultad de Ciencias Químicas, Laboratorio de Biotecnología. Av. Universidad S/N Ciudad Universitaria, San Nicolás de los Garza, Nuevo León. 66455. México.

[c]Università degli Studi di Modena e Reggio Emilia, Dipartimento di Ingegneria "Enzo Ferrari", Via P. Vivarelli 10/1 41125, Italia.

[*]Corresponding author: Tel.: +52 8126531301; mariacamila.arizat@gmail.com

ABSTRACT

Currently, the global community considers microplastics as a marine pollutant of emerging concern. To mitigate the oceanic microplastic pollution, it is necessary to reduce inputs from inland. In this sense, we present the first report on the use of photocatalysis for the degradation of HDPE microplastics extracted from a commercially available facial scrub. This was achieved by using two proposed semiconductors based on N-TiO_2. One was green synthesized using the extrapallial fluid of fresh blue mussels, which presented an excellent capacity to promote photocatalytic degradation in solid and aqueous environments; while the second photocatalyst, obtained from a conventional sol-gel synthesis, presented good capacity to promote mass loss of the as-extracted microplastics in an aqueous environment. Mass losses, SEM and FTIR analysis confirmed HDPE degradation.

Results showed that environmental conditions, microplastics/N-TiO_2 interaction and the N-TiO_2 surface area should be carefully set and monitored in order of avoiding the arrest of photocatalysis.

Keywords:

Films (A), Composites (B), N-TiO_2 (D), Functional applications (E), microplastics.

1. INTRODUCTION

Plastics are synthetic organic polymers which result from the polymerization between monomers derived from oil and gas [1]. Due to their wide range of physical and chemical properties, durability and relatively low cost, plastics are considered ideal materials with an extensive variety of applications by many industries [2,3]. For example, the manufacturing industry uses million tons of plastic per year to produce textile fibers; while the food industries use plastic for packaging products, enabling to reduce food wastage and transportation costs [2]. The economic advantages generated by plastics has caused this industry to grow steadily over the last decades, where world plastic production increased from 1.5 million tons in 1950 to 380 million tons in 2016 [3].

Despite the benefits of plastics to the economy and the daily life of the population, these tend to accumulate in the environment due to their durability and lack of biodegradation [4]. These main intrinsic factors, in addition to their inadequate disposition, are the primary reasons why plastic waste has become a pollution problem of global scale [5]. Initial concerns about contamination by plastics were that 79% of all plastics were being dropped to landfills or illegal dumping sites [6]. However, nowadays we know the pollution problem does not necessarily finish there. Plastics can migrate along the environment throughout rivers ending in freshwater bodies such as lakes and lagoons, or even seas and oceans, where they can reach distant parts of the world as they can travel through marine currents [7]. Recent studies warn there may be as much as 5.3 trillion plastic

particles currently floating on the sea, which is equivalent to 268,940 tons [8]. These have been found to be comprised of all the variety of plastics used by our communities, including polyethylene (PE), polypropylene (PP), polyvinyl chloride (PVC), polyester and nylon [9–11]. However, the presence of significant proportions of PE micro-debris (< 5mm) has attracted particular attention due to the physical damage that poses to marine biota and the increasing hazard that represents to public health [12].

PE micro-debris can be derived from two primary sources, which are defined as primary or secondary according to their origin. In general, primary microplastics are manufactured to be used in facial-cleansers and cosmetics, synthetic clothing, and abrasives found in cleaning products. On the other hand, secondary microplastics are described as tiny plastic fragments derived from the breakdown of larger plastic debris [13]. Despite their origin, remotion of PE microplastics from the oceans represents a difficult task, mainly due to their small size and their continuous breakdown evolution. To date, measures focused on reducing inputs from inland are widely recognized as being the most effective way to mitigate the oceanic microplastic pollution [14,15].

In this regard, we propose the use of photocatalysis to degrade PE microplastics as a promising alternative to minimize its introduction rate to the oceans from continental sources. This was achieved in a sustainable process as the PE was degraded by an N-TiO_2 photocatalyst exposed to visible light. In general, photocatalytic degradations occurs when a semiconductor is exposed to a source of light emitting photons with equal or higher energy than its band gap, causing the generation of holes (h^+) and excited electrons (e^-) [16]. These holes, combined with water (H_2O) or hydroxyl groups (OH^-), generating hydroxyl radicals ($OH^\bullet$) which are highly oxidizing species capable of degrading different organic pollutants [16]. To achieve a more sustainable process, our N-TiO_2 semiconductor was prepared following the procedure reported by Zeng et al. [17], where an N-doped TiO_2 semiconductor is obtained by a synthesis inspired in a bioprocess using mussel proteins as pore-forming agent and nitrogen source for the photocatalyst doping.

In this study, we present the photocatalytic degradation of real samples of PE microplastics extracted from a commercially available facial scrub, one of the products that have been suggested as a significant source of marine microplastics [18]. The degradation of this active ingredient under visible light was achieved by two proposed methodologies, which were performed in either aqueous and solid matrix to demonstrate the adaptability and applicability of this strategy. While photocatalytic degradation was confirmed to occur faster in an aqueous medium, conditions should be carefully chosen and furtherly investigated, since photocatalysis of PE was arrested in both media after irradiation for long periods of time.

2. MATERIALS AND METHODS

2.1. Synthesis and characterization of N-TiO_2 semiconductors

The green synthesis of an N-TiO_2 semiconductor was adapted from Zeng et al. [17]. Briefly, the extrapallial fluid of fresh blue mussels (*Mytilus edulis*) collected from Ensenada, Mexico (31.8667° N, 116.5964° W) was centrifuged at 13,000 rpm for 10 minutes using an Eppendorf 5415D centrifuge. The cleared extrapallial fluid was used as a pore-forming agent and nitrogen precursor in the preparation of the visible-active N-TiO_2 semiconductor by dropping 5 mL into 1 mL of titanium (IV) butoxide (Sigma-Aldrich, 97%) and mixing it for 2 h at 300 rpm. Mineralization of the mixture was performed at room temperature for 4 h. The mixture was transferred into a Teflon-lined autoclave and subjected to thermal treatment, using an initial thermal stage at 50 ºC for 30 min, followed by a second one at 150 ºC for 12 h with a heating rate of 5 ºC/min. The resulting powders were filtered, washed with distilled water and dried at 55 ºC.

The total protein concentration in the cleared extrapallial fluid was determined using the Bradford assay [19] using a Cary 50 UV-Vis spectrophotometer from Agilent Technologies.

The synthesis of a second N-TiO_2 material to be used as a control was prepared by the traditional sol-gel method using urea (Analytyca, reagent grade) as a nitrogen precursor and tri-block copolymer (Pluronic® F-127, Sigma-Aldrich) as a pore-forming agent. Briefly, the precursor solution was prepared by the slow addition of 1 mL of $TiCl_4$ (Sigma-Aldrich, 99.9%) to a mixture of 20 mL of absolute ethanol (DEQ, 99.8%) and 570 mg of Pluronic® F-127. Then, 1.65 mL of ultrapure water (18 MΩ) was added drop-by-drop and stirred for 5 min. Finally, 73 mg of urea were added to the mixture. The film was prepared by pouring the precursor solution into the Batch reactor walls and thermally treated at 200°C for 24 h and 500°C for 3 h to crystallize the anatase TiO_2 phase.

Characterization of the crystalline phase in both N-TiO_2 materials was achieved by X-ray diffraction, using a Siemens D5000 diffractometer with Cu Kα1 radiation. Nitrogen incorporation into the TiO_2 network was verified using a Vertex 70 ATR-FTIR Bruker spectrometer by averaging 32 scans between 4000 and 400 cm^{-1} with a 4 cm^{-1} spectral resolution. The band gap (E_g) values of the photocatalysts were calculated from their Diffuse reflectance spectra (DRS). Measures were carried out in the 300-800 nm range on a Jasco V-670 UV-Vis/NIR spectrophotometer equipped with a ILN-725 integration sphere. Using the Kubelka-Munk theory, the E_g values were obtained from the intersection of a straight line from the linear region with the abscissa axis of a plot $(F(R)*h\nu)^{1/2}$ vs. $h\nu$ in eV [20]. Microstructural characterization and the film thickness were observed by scanning electron microscopy (SEM), using a Thermo-Fisher Scientific FEI Quanta 200 ESEM.

2.2. Microplastic extraction and characterization

Microplastics were extracted from a commercially available exfoliating scrub following the procedure reported by Napper et al. [18]. Briefly, 60 g of the product were mixed with 500 mL of distilled boiling water. The warm mixture was filtered using a cloth filter with a 500 µm pore size. The resulting microplastics were repeatedly washed with distilled water, dried at 30 ºC for 24 h and stored until use. The microplastics´ morphology was observed by SEM, while their particle size was

measured by optical microscopy using a Leica EZ4 stereomicroscope. Finally, microplastics´ composition was characterized by ATR-FTIR.

2.3. Microplastic photocatalytic degradation

The photocatalytic experiments performed with the mussel-derived N-TiO_2 powders were carried using microplastics/N-TiO_2 film composites. These latter were prepared by dissolving 200 mg of the extracted microplastics into 30 mL of cyclohexane (Sigma-Aldrich, 99.6%). The mixture was heated at 70ºC with stirring (300 rpm) for 10 min. After dissolution, 10 mg (the same estimated mass than the deposited N-TiO_2 film) of the mussel-derived N-TiO_2 powders were added, and stirring was allowed for 15 min. The mixture was dried at 55ºC for 20 min and then, allowed to dry at room temperature for 48 hours. The photocatalytic experiments carried out with the control sample (sol-gel N-TiO_2) were performed by directly adding 200 mg of the extracted microplastics and 100 mL of distilled water into the N-TiO_2-coated Batch Reactor.

All the photocatalytic tests were performed in a closed reaction chamber at room temperature for 20 h, with samples placed at 120 mm of a 27 W fluorescent lamp with constant light emissions in the visible spectrum (400 nm – 800 nm, measured with an Ocean Optics USB200 spectrometer). Photocatalysis of microplastics/N-TiO_2 film composites was evaluated *1)* in solid form at room temperature and 50% relative humidity; and *2)* in an aqueous medium using distilled water at 25 ºC. The photocatalysis performed in the sol-gel N-TiO_2-coated Batch reactor was performed only in aqueous medium at 25 ºC. The same experiments were performed in the dark to determine whether the contact between microplastics and N-TiO_2 promotes degradation when no photons are involved in the process. Light exposure of the microplastics without the N-TiO_2 was also performed to test photolysis. All the tests were performed in duplicates with no significant differences observed.

Plastic degradation was measured by weight loss [21–27], with chemical and morphological changes confirmed by FTIR and SEM. Mass loss was calculated using the following equation:

Mass loss (%) = $(M_0 - M)/M_0 \times 100$ Eq. (1)

where M_0 is the initial mass of the microplastics and M is the mass at t hours of irradiation. First-order degradation kinetics were calculated using equation 2:

$C = C_0 \cdot \exp^{-kt}$ Eq. (2)

where C_0 is the initial concentration of microplastics, C is the concentration at time t and k is the first order rate constant [28]. Rate constants were obtained by plotting ln C/C_0 *vs.* t.

3. RESULTS AND DISCUSSIONS

3.1. Synthesis and characterization of N-TiO_2 semiconductors

As shown in **Figure 1,** both N-TiO_2 materials were synthesized in the anatase crystalline phase, which is known to be responsible for the photocatalytic activity of the material [29]. The sol-gel N-TiO_2 film presented higher crystallinity than the protein-derived material. This can be attributed to the thermal treatment occurred after the sol-gel process. On the other hand, the protein-derived N-TiO_2 powder presented a single diffraction peak at ca. 45º, attributable to a rutile crystalline phase. The XRD results also suggest the protein-derived N-TiO_2 powder was more amorphous than the sol-gel synthesized N-TiO_2.

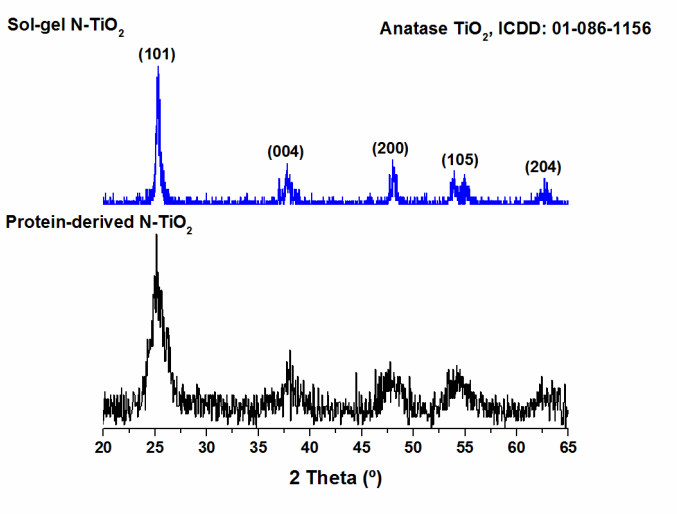

Figure 1. XRD patterns of the sol-gel and protein-derived N-TiO_2 semiconductors.

The ATR-FTIR spectra of both materials exhibited similar bands, confirming the presence of TiO_2 and the incorporation of nitrogen into the semiconductor network (**Figure 2**). The band observed at 702 cm^{-1} corresponded to the Ti-O stretching and Ti-O-Ti bridging stretching bonds [30,31]; while the band observed at 1630 cm^{-1} corresponded to the bending vibrations of the O-H and N-H bonds [31]. These bands were more prominent in the protein-derived material. This characteristic could result from the combination of two factors: (i) the process by which this sample was synthesized, were powder remained dispersed in the synthesis matrix and (ii) the dryness of the sol-gel derived N-TiO_2 film due to calcination at 500 ºC. The bands observed at 1080 cm^{-1} and 1450 cm^{-1} have been attributed to the vibrations of the Ti-N bond [31,32], confirming that protein concentrations from mussels´extrapallial fluids as low as 10 µg/mL, can be used to dope TiO_2 successfully.

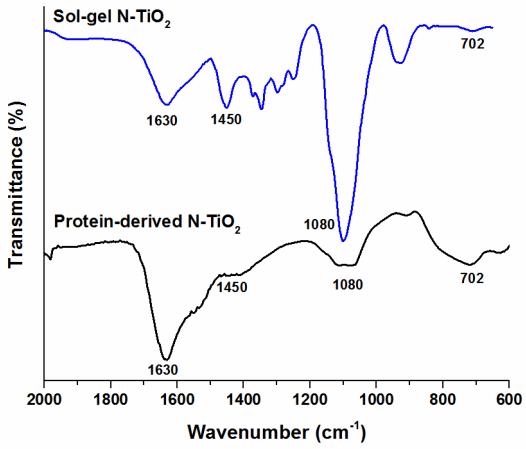

Figure 2. ATR-FTIR spectra of the sol-gel and protein-derived N-TiO_2 semiconductors.

Incorporation of N into the TiO_2 network was also confirmed by the band gap values, which were calculated for both materials (See Supplementary Material). **Table 1** shows that synthesized materials have lower E_g values than the one reported for commercial TiO_2 (3.3 eV [33]), confirming their photocatalytic activity under visible light. Interestingly, mussels-derived N-TiO_2 presented a lower E_g value, suggesting its capability to absorb photons at 427 nm.

Table 1. Absorption properties of the N-TiO_2 photocatalysts.

Sample	Eg (eV)	Wavelength of photon absorption (nm)
Control (sol-gel) N-TiO_2	3.1	400
Protein-derived N-TiO_2	2.9	427

As observed in **Figure 3a**, the sol-gel N-TiO_2 film was composed of particles between 5 and 10 nm of diameter. Porosity, derived from the thermal degradation of the micelles formed by the tri-block copolymer during the synthesis procedure, was uniformly distributed along the sample with

diameters between 2 and10 nm. The film thickness was measured as 975 ± 140 nm. On the other hand, the protein-derived N-TiO_2 powders were observed as agglomerated particles of variable diameters, ranging from 220 to 920 nm (**Figure 3b**). Porosity in the protein-derived N-TiO_2 was present, but it was less distributed than in the sol-gel derived material. This is attributable to the low protein content of the extrapallial fluid used in our work, as the protein concentration used by Zeng and collaborators for the synthesis of their protein-derived N-TiO_2 (600 µg/mL) resulted in the existence of evenly distributed pores along the material [17]. Therefore, although the ATR-FTIR and E_g results showed that low protein content is enough to incorporate nitrogen into the anatase network, our results confirm that lower content of proteins derives in limited porosity, and consequently, a limited surface area on the resultant material.

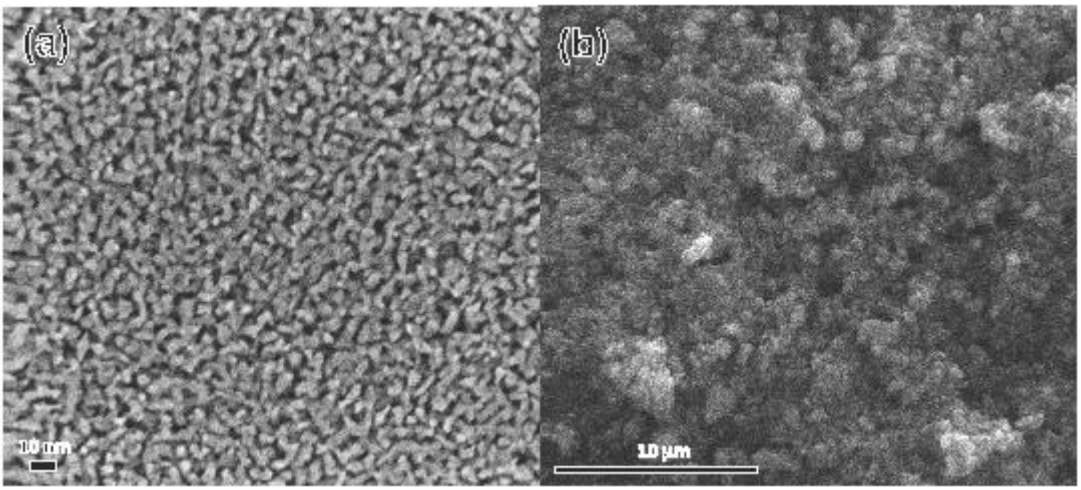

Figure 3. FE-SEM micrographs of the (a) sol-gel and (b) protein-derived N-TiO_2 semiconductors.

3.2. Microplastic extraction and characterization

Blue spherical beads constituted the microplastics extracted from the facial scrub with diameters ranging between 700 and 1000 µm (**Figure 4)**.

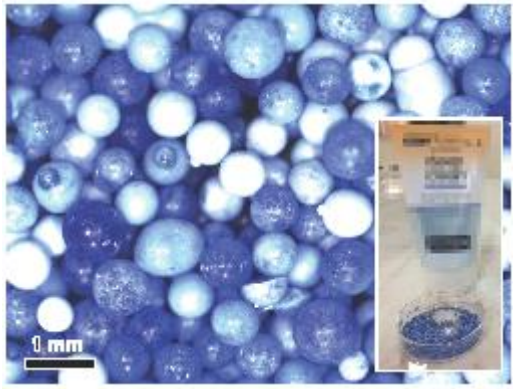

Figure 4. Optic micrograph of the extracted microplastics (16x). Inset: microplastics extracted from the commercially available facial scrub.

The ATR-FTIR analysis confirmed the presence of absorption bands at 2925, 2840, 1467 and 720 cm^{-1} (**Figure 5a**), which are characteristic of the long alkyl chains that compose the high-density polyethylene (HDPE) [33]. On the other hand, the XRD pattern (**Figure 5b**) exhibited the peaks corresponding to the (110), (200), (210) and (020) reflection planes of the orthorhombic unit cell structure of HDPE [34], therefore, confirming the identity of the extracted microplastics.

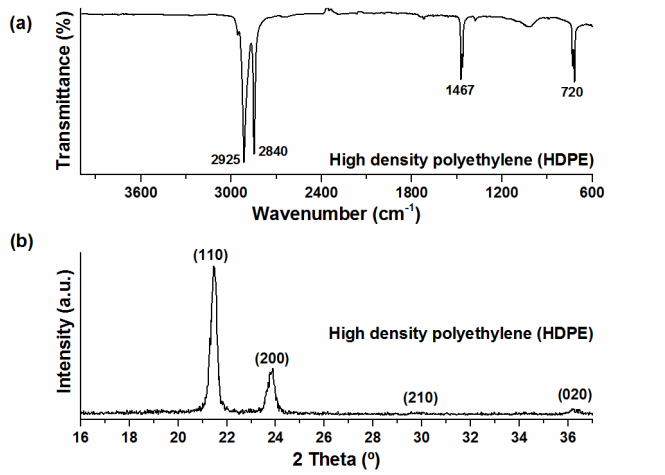

Figure 5. (a) ATR-FTIR spectrum and (b) XRD pattern of the extracted microplastics.

3.3. Microplastic photocatalytic degradation

Figure 6a shows the experiments performed in solid form at room temperature and 50% relative humidity. The photolysis (black curve) demonstrated that HDPE films subjected to visible light for 20 hours did not present significant changes in mass weight, suggesting that HDPE polymers do not degrade under natural environmental conditions. The same experiment carried out with the addition of the protein-derived N-TiO_2 without light irradiation is shown in the pink curve of **Figure 6a**. No mass loss was detected, proving that degradation cannot proceed without photon absorption by the semiconductor. However, with illumination, changes in the microplastic mass were observed during the first 16 h of irradiation, resulting in a total mass loss of 1.85% (blue curve of **Figure 6a**). Since mass losses from N-TiO_2 are not expected under these testing conditions, the resulting mass loss reported in this experiment was attributed to microplastic photocatalytic degradation. Interestingly, as shown in **Figure 6a**, a slow but continuous mass loss in HDPE was observed when the composite was irradiated between 2 and 8 h, achieving a mass loss of 0.75%. However, an arrest on the photocatalysis was observed during the next 4 h of experimentation. This arrest was associated with dehydration of the sample, as previous studies have demonstrated that plastic degradation driven by photocatalysis is commonly carried out by hydroxyl radicals [35–38]. Since these are mainly generated by water adsorbed in the semiconductor surface, a good hydration state of the photocatalyst is fundamental to achieve the degradation of the microplastic [16,36,39]. As in this experiment, HDPE photocatalysis was conducted at room humidity without a continuous source of humidity to the reaction chamber, it is very likely that the composite became dehydrated after 8 h of irradiation. To prove this hypothesis, the reaction chamber was opened to allow the introduction of humidity from the ambient air into the chamber. The photocatalytic test was allowed to continue, and an immediate restoration in the mass loss of the HDPE was observed, reaching a percentage of 1.1% before the second arrest on photocatalysis after 4 hours of additional irradiation. Thus, it was confirmed that humidity is essential for plastic photocatalytic degradation.

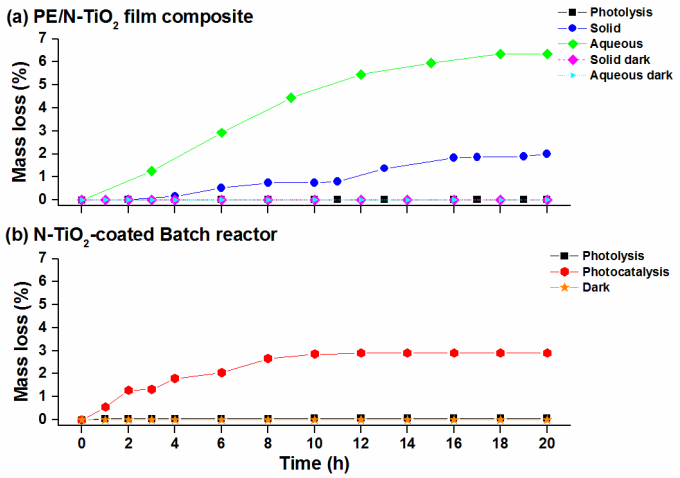

Figure 6. Photocatalytic degradation of HDPE microplastics using N-TiO_2 semiconductors and a 27 W fluorescent visible light (400 - 800 nm).

Moreover, the photodegradation of HDPE by N-TiO_2 was also associated with the porosity of the material. As observed in **Figure 7,** SEM micrographs of the HDPE/N-TiO_2 composite before and after photocatalysis exhibit limited dispersion of N-TiO_2 powders into the composite film, resulting in sparsely distributed cavities in the composite film formed as consequence of the photocatalytic degradation [28,33]. This result confirms that the contact area between the microplastic and the N-TiO_2 is crucial for the degradation of this pollutant. Therefore, it can be suggested that this interaction can be furtherly improved by increasing the surface area of the semiconductor (i.e., increasing the protein content during the synthesis of the N-TiO_2 material).

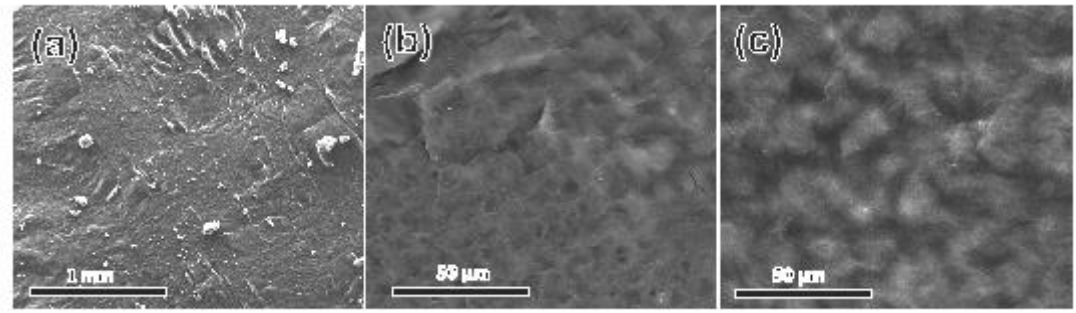

Figure 7. SEM micrographs of the HDPE/N-TiO_2 composites (semiconductor derived from the proteins). (a) As-prepared, (b) solid photocatalysis and (c) aqueous photocatalysis.

The first order kinetic constant was calculated as 12.2 x 10^{-4} h^{-1} (**Table 2**). While the percentage of mass loss on HDPE films can be considered low, it is still higher than those reported for PE plastic photodegradation using TiO_2 or others photocatalysts [28,33,40,41].

Table 2. Calculated first order rate constants.

System	k X 10^{-4} (h^{-1})	R^2
PE/N-TiO_2 composite (solid media)	12.2 ± 0.8	0.9794
PE/N-TiO_2 composite (aqueos media)	38.2 ± 3.7	0.9561
N-TiO_2-coated Batch reactor	27.4 ± 3.3	0.9315

A second photocatalytic test was conducted using the HDPE/N-TiO_2 composite in an aqueous medium at room temperature. Also in this case, in the experiment without irradiation mass loss was not detected (cyan curve of **Figure 6a**). On the other hand, the same system presented an increasing mass loss during the first 18 h of visible irradiation, followed by the arrest of the photocatalysis (green curve of **Figure 6a**). The mass loss was calculated as 6.40%, with a kinetic constant three times faster than the photocatalytic degradation in the solid phase (**Table 2**). This can be associated with the higher concentration of hydroxyl radicals available for degradation in the aqueous solution, as radicals may have been derived from the water adsorbed in the N-TiO_2 surface. SEM analysis confirmed the degradation of HDPE, as voids can be observed along the surface of the composite film (**Figure 7c**). Therefore, our results suggest that protein-derived N-

TiO_2 was able to degrade HDPE plastic in both aqueous and solid media under naturally occurring conditions. Nevertheless, these and pollutant/N-TiO_2 interaction should be carefully set and designed to avoid arrests on the photocatalysis.

To determine the feasibility of this technology for the degradation of microplastics, a degradation test using as-extracted microplastics was performed in an aqueous medium using a Batch reactor (**Figure 6b**). The photolysis experiment in the un-coated Batch reactor demonstrated that as-extracted microplastics do not experience photolysis after 20 h of visible irradiation (black curve). The test in the dark using the N-TiO_2-coated reactor presented the same trend (orange curve). However, illumination of the system promoted the photocatalytic degradation of the microplastics (red curve). A mass loss of 2.86% was achieved after 8 h of irradiation with a kinetic rate constant of 27.4 X 10^{-4} h^{-1} (**Table 2**). These parameters were in between the results observed for the solid and aqueous photocatalysis performed on the composites. **Figure 8** shows the ATR-FTIR spectra of the microplastics before and after photocatalysis, as deducted from the reduction of the characteristic bands of HDPE, the disappearing of microplastics can be confirmed.

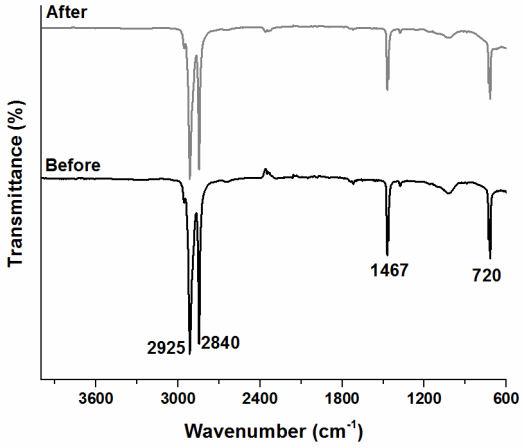

Figure 8. ATR-FTIR spectra of the HDPE microplastics before and after photocatalysis in the Batch Reactor.

CONCLUSIONS

In this work, the photocatalytic degradation of microplastics was conducted using N-TiO_2. The more sustainable N-TiO_2, derived from the extrapallial fluid of saltwater mussels, presented an excellent capacity to promote mass loss of HDPE microplastics in the solid and aqueous environment. The other photocatalyst, derived from a conventional less sustainable sol-gel route, also presented good capacity to promote mass loss of the as-extracted microplastics in an aqueous environment. Results showed that the environmental conditions (those that promote water adsorption into the N-TiO_2), the pollutant/N-TiO_2 interaction and the photocatalyst surface area should be carefully set or designed in order of avoiding the arrest of photocatalysis. The Batch tests revealed that photocatalysis of HDPE microbeads should be further investigated and adapted for application in domestic wastewater treatment plants. Currently, our research group is carrying out investigations to determine the degradation paths of the PE microplastics and the optimal conditions to scale this technology.

ACKNOWLEDGEMENTS

This work was supported by UANL's *Programa de Apoyo a la Investigación Científica y Tecnológica (PAICYT)* [Grant number IT691-18, 2018]. Special thanks are also given to Aranza Denisse Vital Grappin, Rodolfo García Cortés and Luis Enrique Cruz Ruiz, bachelor students from the Facultad de Ciencias Químicas (UANL), for their help with performing some experiments.

COMPETING INTERESTS

The authors declare no competing financial interests.

REFERENCES

[1] M. Cole, P. Lindeque, C. Halsband, T.S. Galloway, Microplastics as contaminants in the marine environment: A review, Mar. Pollut. Bull. 62 (2011) 2588–2597. doi:10.1016/j.marpolbul.2011.09.025.

[2] A.L. Andrady, M.A. Neal, Applications and societal benefits of plastics, Philos. Trans. R. Soc. B Biol. Sci. 364 (2009) 1977–1984. doi:10.1098/rstb.2008.0304.

[3] PlasticsEurope, Plastics-the Facts 2017 An analysis of European plastics production, demand and waste data, Brussels, 2017. https://www.plasticseurope.org/application/files/5715/1717/4180/Plastics_the_facts_2017_FINAL_for_website_one_page.pdf (accessed July 26, 2018).

[4] GESAMP, Sources, Fate and Effects of Microplastics in the Marine Environment: Part 2 of a Global Assessment, Reports Stud. Jt. Gr. Expert. Sci. Asp. Mar. Environ. Prot. Eng No. 93. (2016).

[5] United Nations Environment Programme (UNEP), Marine plastic debris and microplastics – Global lessons and research to inspire action and guide policy change, (2016). doi:10.2173/bna.44.

[6] R. Geyer, J.R. Jambeck, K.L. Law, Production, use, and fate of all plastics ever made, Sci. Adv. 3 (2017) e1700782. doi:10.1126/sciadv.1700782.

[7] N.H. Golden, S.E. Warner, M.J. Coffey, Reviews of Environmental Contamination and Toxicology Volume 237, 237 (2016) 123–191. doi:10.1007/978-3-319-23573-8.

[8] M. Eriksen, L.C.M. Lebreton, H.S. Carson, M. Thiel, C.J. Moore, J.C. Borerro, F. Galgani, P.G. Ryan, J. Reisser, Plastic Pollution in the World's Oceans: More than 5 Trillion Plastic Pieces Weighing over 250,000 Tons Afloat at Sea, PLoS One. 9 (2014) e111913. doi:10.1371/journal.pone.0111913.

[9] S.S. Sadri, R.C. Thompson, On the quantity and composition of floating plastic debris entering and leaving the Tamar Estuary, Southwest England, Mar. Pollut. Bull. 81 (2014) 55–60. doi:10.1016/j.marpolbul.2014.02.020.

[10] S. Sruthy, E. V Ramasamy, Microplastic pollution in Vembanad Lake, Kerala, India: The first report of microplastics in lake and estuarine sediments in India, Environ. Pollut. 222 (2017) 315–322. doi:10.1016/j.envpol.2016.12.038.

[11] K. Zhang, J. Su, X. Xiong, X. Wu, C. Wu, J. Liu, Microplastic pollution of lakeshore sediments from remote lakes in Tibet plateau, China, Environ. Pollut. 219 (2016) 450–455. doi:10.1016/j.envpol.2016.05.048.

[12] N. Weithmann, J.N. Möller, M.G.J. Löder, S. Piehl, C. Laforsch, R. Freitag, Organic fertilizer as a vehicle for the entry of microplastic into the environment, Sci. Adv. 4 (2018) eaap8060. doi:10.1126/sciadv.aap8060.

[13] H.S. Auta, C.U. Emenike, S.H. Fauziah, Distribution and importance of microplastics in the marine environmentA review of the sources, fate, effects, and potential solutions, Environ. Int. 102 (2017) 165–176. doi:10.1016/j.envint.2017.02.013.

[14] D. Eerkes-Medrano, R.C. Thompson, D.C. Aldridge, Microplastics in freshwater systems: A review of the emerging threats, identification of knowledge gaps and prioritisation of research needs, Water Res. 75 (2015) 63–82. doi:10.1016/j.watres.2015.02.012.

[15] United Nations Environment Programme, Global Programme of Action, Open University of the Netherlands, MOOC sobre basura Marina, (2018).

[16] E.I. Cedillo-González, R. Riccò, S. Costacurta, C. Siligardi, P. Falcaro, Below room temperature : how the photocatalytic activity of dense and mesoporous TiO_2 coatings is affected, Appl. Surf. Sci. 435 (2018) 769–775. doi:10.1016/J.APSUSC.2017.11.078.

[17] H. Zeng, J. Xie, H. Xie, B. Su, M. Wang, H. Ping, Bioprocess-inspired synthesis of hierarchically porous nitrogen-doped TiO_2 with high visible-light photocatalytic activity, J. Mater. Chem. A Mater. Energy Sustain. 3 (2015) 19588–19596. doi:10.1039/C5TA04649A.

[18] I.E. Napper, A. Bakir, S.J. Rowland, R.C. Thompson, Characterisation, quantity and sorptive properties of microplastics extracted from cosmetics, Mar. Pollut. Bull. 99 (2015) 178–185. doi:10.1016/j.marpolbul.2015.07.029.

[19] M.M. Bradford, A rapid and sensitive method for the quantitation of microgram quantities of

protein utilizing the principle of protein-dye binding, Anal. Biochem. 72 (1976) 248–254. doi:10.1016/0003-2697(76)90527-3.

[20] A. Cordero-García, G. Turnes Palomino, L. Hinojosa-Reyes, J.L. Guzmán-Mar, L. Maya-Teviño, A. Hernández-Ramírez, Photocatalytic behaviour of WO_3/TiO_2-N for diclofenac degradation using simulated solar radiation as an activation source, Environ. Sci. Pollut. Res. 24 (2017) 4613–4624. doi:10.1007/s11356-016-8157-0.

[21] S. Li, S. Xu, L. He, F. Xu, Y. Wang, L. Zhang, Photocatalytic degradation of polyethylene plastic with polypyrrole/TiO_2 nanocomposite as photocatalyst, Polym. - Plast. Technol. Eng. 49 (2010) 400–406. doi:10.1080/03602550903532166.

[22] R.T. Thomas, V. Nair, N. Sandhyarani, TiO_2 nanoparticle assisted solid phase photocatalytic degradation of polythene film: A mechanistic investigation, Colloids Surfaces A Physicochem. Eng. Asp. 422 (2013) 1–9. doi:10.1016/j.colsurfa.2013.01.017.

[23] T.J. Kemp, R.A. McIntyre, Influence of transition metal-doped titanium(IV) dioxide on the photodegradation of polystyrene, Polym. Degrad. Stab. 91 (2006) 3010–3019. doi:10.1016/j.polymdegradstab.2006.08.005.

[24] X.U. Zhao, Z. Li, Y. Chen, L. Shi, Y. Zhu, Solid-phase photocatalytic degradation of polyethylene plastic under UV and solar light irradiation, J. Mol. Catal. A Chem. 268 (2007) 101–106. doi:10.1016/j.molcata.2006.12.012.

[25] R.T. Thomas, N. Sandhyarani, Enhancement in the photocatalytic degradation of low density polyethylene-TiO_2 nanocomposite films under solar irradiation, RSC Adv. 3 (2013) 14080–14087. doi:10.1039/c3ra42226g.

[26] X. Zhao, Z. Li, Y. Chen, L. Shi, Y. Zhu, Enhancement of photocatalytic degradation of polyethylene plastic with CuPc modified TiO_2 photocatalyst under solar light irradiation, Appl. Surf. Sci. 254 (2008) 1825–1829. doi:10.1016/j.apsusc.2007.07.154.

[27] L. Zan, W. Fa, S. Wang, Novel photodegradable low-density polyethylene-TiO_2 nanocomposite film, Environ. Sci. Technol. 40 (2006) 1681–1685. doi:10.1021/es051173x.

[28] S.S. Ali, I.A. Qazi, M. Arshad, Z. Khan, T.C. Voice, C.T. Mehmood, Photocatalytic

degradation of low density polyethylene (LDPE) films using titania nanotubes, Environ. Nanotechnology, Monit. Manag. 5 (2016) 44–53. doi:10.1016/j.enmm.2016.01.001.

[29] T. Luttrell, S. Halpegamage, J. Tao, A. Kramer, E. Sutter, M. Batzill, Why is anatase a better photocatalyst than rutile? - Model studies on epitaxial TiO_2 films, Sci. Rep. 4 (2015) 4043. doi:10.1038/srep04043.

[30] G. Socrates, Infrared and Raman Characteristic Group Frequencies : Tables and Charts, 3rd ed., John Wiley & Sons, 2004.

[31] G. Yang, Z. Jiang, H. Shi, T. Xiao, Z. Yan, Preparation of highly visible-light active N-doped TiO_2 photocatalyst, J. Mater. Chem. 20 (2010) 5301. doi:10.1039/c0jm00376j.

[32] Y. huo, Y. Jin, J. Zhu, H. Li, Highly active $TiO_{2-x-y}N_xF_y$ visible photocatalyst prepared under supercritical conditions in NH_4F/EtOH fluid, Appl. Catal. B Environ. 89 (2009) 543–550. doi:10.1016/j.apcatb.2009.01.019.

[33] G. Liu, D. Zhu, W. Zhou, S. Liao, J. Cui, K. Wu, D. Hamilton, Solid-phase photocatalytic degradation of polystyrene plastic with goethite modified by boron under UV-vis light irradiation, Appl. Surf. Sci. 256 (2010) 2546–2551. doi:10.1016/j.apsusc.2009.10.102.

[34] F. Chouit, O. Guellati, S. Boukhezar, A. Harat, M. Guerioune, N. Badi, Synthesis and characterization of HDPE/N-MWNT nanocomposite films, Nanoscale Res. Lett. 9 (2014) 288. doi:10.1186/1556-276X-9-288.

[35] J.M. Coronado, M.E. Zorn, I. Tejedor-Tejedor, M.A. Anderson, Photocatalytic oxidation of ketones in the gas phase over TiO_2 thin films: a kinetic study on the influence of water vapor, Appl. Catal. B Environ. 43 (2003) 329–344. doi:10.1016/S0926-3373(03)00022-5.

[36] T.N. Obee, R.T. Brown, TiO_2 Photocatalysis for Indoor Air Applications: Effects of Humidity and Trace Contaminant Levels on the Oxidation Rates of Formaldehyde, Toluene, and 1,3-Butadiene, Environ. Sci. Technol. 29 (1995) 1223–1231. doi:10.1021/es00005a013.

[37] C. Raillard, V. Héquet, P. Le Cloirec, J. Legrand, Kinetic study of ketones photocatalytic oxidation in gas phase using TiO_2-containing paper: Effect of water vapor, J. Photochem. Photobiol. A Chem. 163 (2004) 425–431. doi:10.1016/j.jphotochem.2004.01.014.

[38] L.A. Dibble, G.B. Raupp, Kinetics of the gas-solid heterogeneous photocatalytic oxidation of trichloroethylene by near UV illuminated titanium dioxide, Catal. Letters. 4 (1990) 345–354. doi:10.1007/BF00765320.

[39] A. Mills, A. Lepre, N. Elliott, S. Bhopal, I.P. Parkin, S.A. O'Neill, Characterisation of the photocatalyst Pilkington Activ^{TM}: A reference film photocatalyst?, J. Photochem. Photobiol. A Chem. 160 (2003) 213–224. doi:10.1016/S1010-6030(03)00205-3.

[40] G.L. Liu, D.W. Zhu, S.J. Liao, L.Y. Ren, J.Z. Cui, W.B. Zhou, Solid-phase photocatalytic degradation of polyethylene-goethite composite film under UV-light irradiation, J. Hazard. Mater. 172 (2009) 1424–1429. doi:10.1016/j.jhazmat.2009.08.008.

[41] G. Liu, S. Liao, D. Zhu, J. Cui, W. Zhou, Solid-phase photocatalytic degradation of polyethylene film with manganese oxide OMS-2, Solid State Sci. 13 (2011) 88–94. doi:10.1016/j.solidstatesciences.2010.10.014.